

Self-organizing Multiagent Target Enclosing under Limited Information and Safety Guarantees

Praveen Kumar Ranjan, Abhinav Sinha, *Member, IEEE*, Yongcan Cao, *Senior Member, IEEE*

Abstract—This paper introduces an approach to address the target enclosing problem using non-holonomic multiagent systems, where agents autonomously self-organize themselves in the desired formation around a fixed target. Our approach combines global enclosing behavior and local collision avoidance mechanisms by devising a novel potential function and sliding manifold. In our approach, agents independently move toward the desired enclosing geometry when apart and activate the collision avoidance mechanism when a collision is imminent, thereby guaranteeing inter-agent safety. We rigorously show that an agent does not need to ensure safety with every other agent and put forth a concept of the nearest colliding agent (for any arbitrary agent) with whom ensuring safety is sufficient to avoid collisions in the entire swarm. The proposed control eliminates the need for a fixed or pre-established agent arrangement around the target and requires only relative information between an agent and the target. This makes our design particularly appealing for scenarios with limited global information, hence significantly reducing communication requirements. We finally present simulation results to vindicate the efficacy of the proposed method.

Index Terms—Multiagent Systems, Target Enclosing, Collision Avoidance, Motion Planning, Safety, Self-organizing Behavior.

I. INTRODUCTION

In recent times, autonomous vehicles have gained significant prominence in a range of tasks, including reconnaissance, surveillance, crop and forest monitoring, and search and rescue missions, e.g., [1]–[5]. Most of these tasks share a common behavior where an autonomous vehicle, known as the pursuer, monitors an object of interest, known as the target. In general, the pursuer’s stable motion around the target by maintaining the desired separation from the target is referred to as target enclosing [6] or encirclement/circumnavigation/entrapment when the enclosing orbit is a circle [7].

One of the earliest approaches for target circumnavigation entails pursuers confining the target in a specific geometric shape posing as a formation control problem. The authors in [8], [9] utilize a cyclic pursuit strategy to cooperatively enclose a target, achieving and maintaining uniform angular spacing among the agents. Vector field guidance is another popular approach, where vector fields can be designed to

create a limit cycle or periodic orbit around the target, guiding agents to desired geometric shapes [10], [11]. However, each orbit may require a separate field, thus limiting its applicability in a multiagent scenario. Several other guidance strategies have also been developed for trapping targets in circular orbits, based on differential geometry [12], model predictive control [13], and reinforcement learning [14]. Many of the works in the target enclosing have focused on reducing the information required for developing the control laws. For example, some strategies utilize only range-only measurements [15]–[17], bearing angle measurement [18], [19], range and bearing information [7], [20], [21]. The general moving target enclosing problem using a single agent was studied in [22], [23], whereas the authors in [24] guided multiple agents to the desired proximity with equal angular spacing. Note that these works did not account for explicit inter-agent safety.

Most studies on target enclosing have focused on ensuring that pursuers reach the target without considering their safety or coordinating their movements with other pursuers. However, this approach can result in collisions between pursuers, which may result in mission failure. To address this issue, some studies have introduced decentralized methods for collision avoidance between pursuers, allowing them to orbit the target while maintaining a safe distance from each other [8], [9], [13], [24]–[26]. However, these methods often rely on strict formations, such as equal angular spacing, which can limit the pursuers’ movement and increase the complexity of the guidance strategy. By eliminating the need for rigid formations and reducing the number of agents that each pursuer must communicate with, we can simplify the guidance strategy and improve its robustness to changes in the number of pursuers in the enclosing formation.

Motivated by the aforementioned studies, our work aims to create efficient target-enclosing guidance laws that do not require extensive information exchange or predefined agent configurations. Our main contributions include developing a distributed guidance law for pursuers to safely enclose a target while avoiding collisions, using a minimal amount of information, and no fixed agent formations. Each pursuer only coordinates with one other pursuer when necessary to prevent collisions, thereby ensuring inter-agent safety. Our approach introduces a novel decision-making protocol for selecting the appropriate pursuer for coordination and designing a guidance strategy to ensure collision avoidance. We design the guidance law based on a custom potential

P. K. Ranjan and Y. Cao are with the Unmanned Systems Lab, Department of Electrical and Computer Engineering, The University of Texas at San Antonio, TX- 78249 USA. Emails: praveen.ranjan@my.utsa.edu, yongcan.cao@utsa.edu.

A. Sinha is with the GALACxIS Lab, Department of Aerospace Engineering and Engineering Mechanics, University of Cincinnati, OH- 45221 USA. Email: abhinav.sinha@uc.edu.

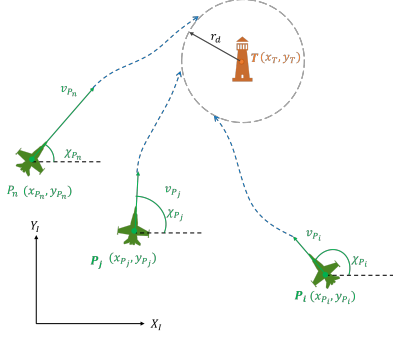


Fig. 1: Target enclosing scenario in the inertial frame of reference.

function that combines attractive and repulsive forces to guide the pursuers toward the desired orbit around the target safely and efficiently. We also demonstrate that our proposed guidance law is robust to the motion of other pursuers and requires only relative information, potentially eliminating the need for costly agent-to-agent communication.

II. PROBLEM FORMULATION

A. Kinematics of Agents' Relative Motions

Consider a multiagent system consisting of n pursuers and a single stationary target T . We use \mathcal{L} to denote the set of the pursuer, that is, $\mathcal{L} = \{P_1, P_2, \dots, P_n\}$. Fig. 1 depicts the engagement geometry between the pursuers and the target, where $[x_i, y_i]^T \in \mathbb{R}^2$ denotes the position of the i^{th} pursuer in the inertial frame of reference, and $\chi_i \in [-\pi, \pi)$ denotes its heading angle. Assuming the vehicles to be point masses, the motion of the i^{th} pursuer is governed by

$$\dot{x}_i = v \cos \chi_i, \quad \dot{y}_i = v \sin \chi_i, \quad \dot{\chi}_i = \frac{a_i}{v},$$

where $v \in \mathbb{R}_{>0}$ denotes the common and constant speed for all pursuers and a_i denotes the lateral acceleration, also the control input, of the i^{th} pursuer. This model, albeit simple, is practical when dealing with vehicles that are turn-constrained and utilize lateral forces (e.g., lift and side force) to maneuver, such as fixed-wing aircraft, missiles, and underwater vehicles [1], [6], [7], [21], [22], [27]. Here we assume that $|a_i| \leq a_i^{\max}$.

The engagement geometry between the vehicles in the relative frame of reference is depicted in Fig. 2, where r_{ij} denotes the distance between the i^{th} and the j^{th} pursuer ($i \neq j$) and accordingly r_{iT} signifies the distance with the target. Similarly, θ_{iT} denotes the line-of-sight (LOS) angle for the i^{th} pursuer with respect to the target and θ_{ij} is the LOS angle between the i^{th} and the j^{th} pursuer referenced from the i^{th} pursuer. The bearing angle of the i^{th} pursuer with respect to the target is $\sigma_i = \chi_i - \theta_{iT}$. Thus, the kinematics of the relative motion for the multiagent system is given by

$$\dot{r}_{iT} = -v \cos \sigma_i \quad (1a)$$

$$\dot{\theta}_{iT} = -\frac{v \sin \sigma_i}{r_{iT}}. \quad (1b)$$

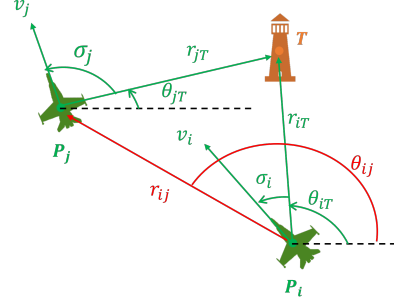


Fig. 2: Target enclosing scenario in the relative frame of reference.

These equations are obtained by projecting the i^{th} pursuer's relative velocities in the directions parallel/normal to the i^{th} pursuer-target LOS.

B. Direction/Sense of Target Enclosing

For the target-centric relative system in (1), r_{iT} is measured from P_i to target and θ_{iT} is measured in a counter-clockwise sense from the horizontal reference. Therefore, positive angular rates pertain to the counter-clockwise revolution of the pursuers about the target. Further, it is evident from (1b) that $\dot{\theta}_{iT} < 0, \forall \sigma_i \in (0, \pi), \dot{\theta}_{iT} > 0, \forall \sigma_i \in (-\pi, 0)$ and $\dot{\theta}_{iT} = 0, \forall \sigma_i \in \{0, \pm\pi\}$.

Remark 1. One may notice from these observations that the i^{th} pursuer revolves around the target in a counter-clockwise direction when $\dot{\theta}_{iT} > 0$ and vice-versa. From the bearing angle relationship, it follows that the positive values of σ_i represent the scenarios when the i^{th} pursuer's heading angle leads the LOS angle in the counter-clockwise direction. Therefore, if σ_i is assumed to be constrained within $(0, \pi)$, then $\dot{\theta}_{iT} < 0$ can be ensured for all $t \geq 0$. This aspect is critical from a safety perspective because it limits the i^{th} pursuer's revolution to the clockwise direction only around the target. This helps ensure that the pursuers do not go in opposite senses while converging on a circle of the same radius, which could lead to a collision.

To describe the relationship between the i^{th} and the j^{th} pursuer at any instant of time in terms of their relative positions, let us define the terms inter-agent separation d_{ij} and the inter-agent angular spacing ψ_{ij} as

$$d_{ij} = r_{iT} - r_{jT}, \quad (2a)$$

$$\psi_{ij} = \theta_{iT} - \theta_{jT}, \quad (2b)$$

where $\psi_{ij} \in [-\pi, \pi)$, as depicted in Fig. 3, where the agents (the pursuers) are enclosing the target in a clockwise direction. In Fig. 3, the dotted circles represent the loiter circles around the target with a radius equal to the instantaneous pursuer-target distance. The positive values of d_{ij} imply that the i^{th} pursuer is on a larger loiter circle compared to the j^{th} pursuer. Hence, $d_{ij} > 0$ implies $\frac{r_{iT}}{r_{jT}} > 1$, and $d_{ij} < 0$ implies that $0 < \frac{r_{iT}}{r_{jT}} < 1$. Similarly, the positive

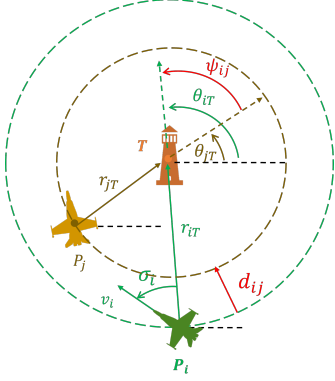


Fig. 3: Inter-agent reference geometry.

values of ψ_{ij} result in a scenario when θ_{jT} leads θ_{iT} in a clockwise sense. The red arrows in Fig. 3 denote the positive conventions of d_{ij} and ψ_{ij} considered in this paper. It is also worth noting that for any two agents P_i and P_j , d_{ij} and ψ_{ij} together represent the inter-agent radial distance r_{ij} . From Fig. 2, using the cosine angle formula from triangle $P_i - P_j - T$, we can obtain the distance between P_i and P_j as, $r_{ij}^2 = r_{iT}^2 + r_{jT}^2 - 2r_{iT}r_{jT} \cos \psi_{ij}$, which reduces to,

$$r_{ij}^2 = 2r_{jT}^2 (1 - \cos \psi_{ij}) + d_{ij}^2 + 2r_{jT}d_{ij} (1 - \cos \psi_{ij}), \quad (3)$$

on using $r_{iT} = r_{jT} + d_{ij}$ from (2a). Hence, if both $d_{ij} \rightarrow 0$ (coincident loiter circles) and $\psi_{ij} \rightarrow 0$ (coincident pursuer-target LOS), then it essentially implies that $r_{ij} \rightarrow 0$, which means inter-agent collision since more than one pursuer occupies the same position.

C. Design of Control Objectives

We aim to make the pursuers organize themselves in a circular orbit around the target while also ensuring that they do not collide with each other, as the orbit is the same for all of them. To solve the multiagent target enclosing problem under limited information and safety constraints, we need to ensure that for each pursuer, starting from any feasible initial conditions, the following holds:

$$\lim_{t \rightarrow \infty} |r_{iT} - r_d| \rightarrow 0, \quad (4)$$

where r_d denotes the fixed desired proximity of the pursuers from the target, which is the same for every pursuer. It is worth noting that fulfilling the objective in (4) is not sufficient to guarantee inter-agent safety because the circular orbit is the same for all pursuers during target enclosing. In addition to (4), the requirement that $r_{ij} > 0, \forall i \neq j$, needs to be satisfied throughout the engagement for safety. This condition ensures that the inter-agent spacing is always greater than a positive value, that is, no two pursuers converge to the same point on the desired enclosing orbit.

Remark 2. As the number of agents increases, exhaustively checking the condition of inter-agent spacing for safety ($r_{ij} > 0$) leads to computational and design complexities in terms of sensing and communication. For an i^{th} agent, there exists

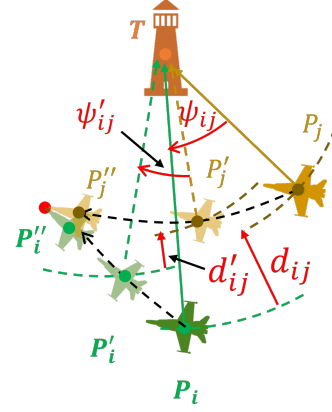


Fig. 4: Engagement between pursuers without safety considerations.

some r_{ij} such that checking their sign to ensure safety would be tedious and redundant. That said, an agent may require extensive sensing and communication with every other agent (not just its neighbors), which may not be efficient.

To elucidate the implications of Remark 2, let us analyze a typical case of target enclosing involving two pursuers, as shown in Fig. 4. If P_j is initially located closer to the target than P_i such that $d_{ij} > 0$ and $\psi_{ij} < 0$, then $\dot{\theta}_{iT} < \dot{\theta}_{jT}$. This essentially means that the component of the relative velocity of P_j normal to r_{jT} is greater than that of P_i , thereby making $\dot{\psi}_{ij} > 0$. This leads to coincident pursuer-target LOS between P_i and P_j at some instant of time during target enclosing. Similarly, the component of the relative velocity of P_j along r_{jT} will be less than that of P_i , thereby making $\dot{d}_{ij} < 0$. This results in the pursuers being on the same loiter circle at some instant of time during target enclosing. Consequently, a collision between P_i and P_j may eventually occur, as demonstrated in Fig. 4, where $(\cdot)'$ and $(\cdot)''$ represent the variables related to the pursuers as time progresses since both $d_{ij} \rightarrow 0$ and $\psi_{ij} \rightarrow 0$ as a result of $\dot{d}_{ij} < 0$ and $\dot{\psi}_{ij} > 0$. Therefore, one may speculate that inter-agent collisions can be prevented if such conditions/scenarios never arise during target enclosing.

The previous analysis showed that collisions between pursuers occur only under specific circumstances. Our method takes advantage of this fact to restrict each pursuer's motion to avoid collisions solely with those pursuers that have the potential to collide in the future. It is important to note that when there are multiple pursuers, several of them may collide with P_i . Consequently, we devise strategies to prevent collisions with a single pursuer while taking into account the potential collisions with all the other pursuers. To this end, we first identify the set of all pursuers that are within the sensing range of the i^{th} pursuer (i.e., $r_{ij} \leq r_s$) and may potentially collide with it. Let us refer to this set as

$$\mathcal{N}_i := \{P_j \in \mathcal{L} \mid d_{ij} > 0 \ \& \ \psi_{ij} < 0\}, \quad \forall i \neq j, \quad (5)$$

which represents the set of all colliding neighbors of P_i . Out

of all such pursuers in \mathcal{N}_i , we identify those pursuers that are situated on a loiter circle whose radius is closest (just smaller) to the one on which P_i is located. Let's define

$$\mathcal{Z}_i := \left\{ P_j \in \mathcal{N}_i \mid d_{ij} = \min_{P_k \in \mathcal{N}_i} d_{ik} \right\}, \quad (6)$$

for any k^{th} pursuer such that $k \neq j$. Note that the sets \mathcal{N}_i and \mathcal{Z}_i may contain more than one pursuer. This happens when multiple neighboring pursuers belonging to the set \mathcal{Z}_i share the same distance from the target. We, however, aim to develop a self-organizing guidance strategy under limited information and safety constraints. This would entail limiting the communication among the pursuers. Toward this objective, we define another set

$$\mathcal{C}_i := \left\{ P_j \in \mathcal{Z}_i \mid \psi_{ij} = \max_{P_k \in \mathcal{N}_i} \psi_{ik} \right\}, \quad (7)$$

that selects only one potentially colliding neighbor from the set \mathcal{Z}_i , thereby allowing us to analyze the behavior of only one pair of pursuers at any instant of time. We refer to the set \mathcal{C}_i as the set of the *nearest colliding pursuer*. In essence, $\mathcal{C}_i \subset \mathcal{Z}_i \subset \mathcal{N}_i$.

Remark 3. Based on the conditions given in (6) and (7), the set \mathcal{C}_i contains at most one neighboring pursuer since a unique combination of (d_{ij}, ψ_{ij}) represents a distinct position of P_j (the nearest colliding pursuer) about P_i . Therefore, it is sufficient to prevent inter-agent collision between any such pair, thereby ensuring safety under limited information.

In this work, we show that if $d_{ij} > 0$ for all $t \geq 0$ in addition to (4), then the pursuers will exhibit a self-organizing behavior during target enclosing while also guaranteeing safety. Ensuring $d_{ij} > 0$ will imply that $r_{ij} > 0$ even if $\psi_{ij} \rightarrow 0$, meaning that every pursuer will maintain a safe distance with respect to every other pursuer in its vicinity.

The scenario represented in Fig. 5 considers three pursuers, P_i , P_j , and P_k aiming to enclose the target within a circle while also ensuring safety. The dotted curves in Fig. 5 represent their instantaneous loiter circles around the target. In this scenario, P_j and P_k initially avoid encountering a nearest colliding pursuer, thus converging to the desired proximity in the same order as they started. Meanwhile, P_i encounters P_j as its nearest colliding pursuer, prompting P_i to maintain $d_{ij} > 0$ to avoid collision with P_j . Subsequently, at a later time during enclosing, $\psi_{ij} \rightarrow 0$, enabling P_i to relax its safety constraint and settle behind P_j , ultimately resulting in collision-free self-organizing target enclosing.

This observation facilitates us to formulate the safety constraint for the i^{th} pursuer as the one of ensuring

$$d_{ij} > 0. \quad (8)$$

This condition guarantees that all pursuers move along a loiter circle with a radius greater than its distance from the nearest colliding pursuer around the target. As a result, $\psi_{ij} \rightarrow 0$, but $d_{ij} \not\rightarrow 0$, which implies that $r_{ij} \not\rightarrow 0$, ensuring that each pursuer keeps a safe distance from its nearest

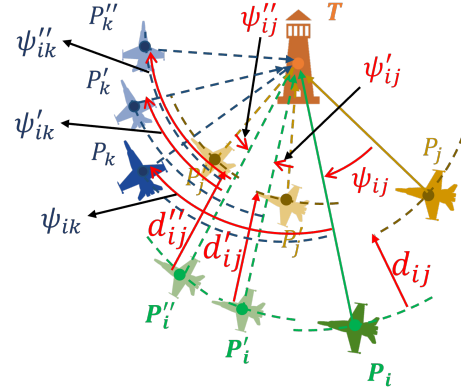


Fig. 5: Multiagent target enclosing scenario with safety constraints.

colliding pursuer and is influenced by at most one other pursuer during enclosing.

Fig. 5 shows the behavior of pursuers who ensure safety conditions in (8), where P_j is the nearest colliding pursuer for P_i . Initially, ψ_{ij} starts at a negative value and becomes positive over time, which is similar to the scenario without safety conditions presented in Fig. 4. However, due to the safety condition, P_i maintains a larger distance from the target than P_j , resulting in a positive d_{ij} . Once $\psi_{ij} = 0$, P_j is no longer the nearest colliding pursuer for P_i , and P_i begins to converge to the desired enclosing geometry while ψ_{ij} becomes increasingly positive. At steady state, P_i autonomously converges to a finite positive value of ψ_{ij} with respect to P_j . This behavior, where pursuers converge to a circle of desired proximity from the target while maintaining a safe distance from each other, is referred to as self-organizing multiagent target enclosing behavior in our paper. Unlike previous works [8], [9], [13], [24]–[26], the safety condition in (8) constrains d_{ij} rather than ψ_{ij} , allowing each pursuer to independently converge to any finite ψ_{ij} with respect to its neighbors. Such behavior enables pursuers to operate without the need for a predetermined formation structure, reducing the amount of information required and coordinating efforts with just one other pursuer, which is the nearest colliding pursuer. This affords pursuers greater autonomy to maneuver independently while still maintaining a stable formation/enclosing geometry. Moreover, pursuers can enter or exit the enclosing formation seamlessly, without disturbing the overall structure.

We are now in a position to summarize the control objectives in regards to the self-organizing multiagent target enclosing under limited information and safety guarantees, that is, $\lim_{t \rightarrow \infty} |r_{iT} - r_d| \rightarrow 0$, and $d_{ij} > 0, \forall P_j \in \mathcal{C}_i$.

III. SELF-ORGANIZING MULTIAGENT TARGET ENCLOSING GUIDANCE LAW WITH INHERENT SAFETY

In this section, we examine the interactions between pursuers and derive the criteria for identifying the nearest colliding pursuer. We then show that satisfaction of the

safety condition in (8) is sufficient for developing a guidance strategy that steers all pursuers on the desired enclosing geometry around the target while also avoiding collisions.

A. Analysis of Inter-Pursuer Behavior

Note that the LOS of the i^{th} pursuer with respect to the target and the line that is normal to it at the i^{th} pursuer's position (the tangent line to its instantaneous loiter circle) partitions the engagement zone into four distinct regions that can be completely characterized using d_{ij} and ψ_{ij} , as shown in Fig. 6. Based on this partition, we can analyze the safety and behaviors of the pursuers as they maneuver to enclose the target. These four distinct region can be characterized as,

$$\begin{aligned} \text{Region I: } d_{ij} > 0, \psi_{ij} > 0, \quad \text{Region II: } d_{ij} \leq 0, \psi_{ij} > 0, \\ \text{Region III: } d_{ij} \leq 0, \psi_{ij} < 0, \quad \text{Region IV: } d_{ij} > 0, \psi_{ij} < 0. \end{aligned} \quad (9)$$

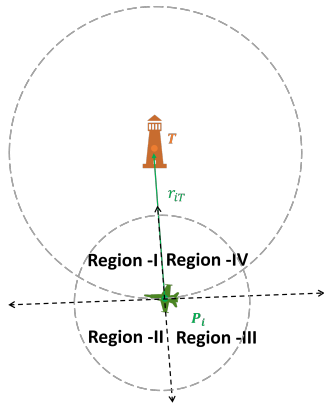


Fig. 6: Regions around the i^{th} pursuer.

Lemma 1. *Pursuers situated in Regions I and III corresponding to the i^{th} pursuer's position do not have a tendency to collide with the i^{th} pursuer.*

Proof. To demonstrate this, we examine the motion of pursuers in the four regions defined in (9) and determine the conditions under which both $d_{ij} \rightarrow 0$ and $\psi_{ij} \rightarrow 0$ can occur. We do this by deriving the dynamics of the inter-pursuer radial distance and inter-pursuer angular spacing, which are given by,

$$\dot{d}_{ij} = -v (\cos \sigma_i - \cos \sigma_j), \quad (10a)$$

$$\dot{\psi}_{ij} = -v \left(\frac{\sin \sigma_i}{r_{iT}} - \frac{\sin \sigma_j}{r_{jT}} \right), \quad (10b)$$

obtained by differentiating (2) with respect to time and using (1). Provided that all pursuers initiate their movement away from the target and tend to move toward it to enclose the latter, we can deduce from (1a) that $\dot{r}_{iT} < 0, \dot{r}_{jT} < 0$. This pertains to the scenario when they are moving toward the target, thus limiting their look angles within the interval $(0, \pi/2)$. Now, if a collision is imminent, then $d_{ij} \rightarrow 0$ and $\psi_{ij} \rightarrow 0$. Let us analyze each of these conditions in the

four regions to analyze the situation when every pursuer is heading toward the target to enclose it.

Using (10a), we can determine the conditions that lead to $d_{ij} \rightarrow 0$ in the four regions as follows:

$$\begin{aligned} \text{Region I: } \dot{d}_{ij} < 0, \text{ if } \sigma_i < \sigma_j, \\ \text{Region II: } \dot{d}_{ij} > 0, \text{ if } \sigma_i > \sigma_j, \\ \text{Region III: } \dot{d}_{ij} > 0, \text{ if } \sigma_i > \sigma_j, \\ \text{Region IV: } \dot{d}_{ij} < 0, \text{ if } \sigma_i < \sigma_j. \end{aligned} \quad (11)$$

Next, we analyze cases when $\psi_{ij} \rightarrow 0$ when the above conditions for $d_{ij} \rightarrow 0$ also hold. We denote σ_i^* as the look angle about which ψ_{ij} changes its sign, given by

$$\sin \sigma_i^* = \frac{r_{iT}}{r_{jT}} \sin \sigma_j, \quad (12)$$

obtained by equating $\dot{\psi}_{ij}$ to zero in (10b).

In Regions I and IV, we have $d_{ij} > 0$ or $\frac{r_{iT}}{r_{jT}} > 1$, which implies $\sigma_i^* > \sigma_j$. Thus, $\sigma_i < \sigma_j$ leads to $\sin \sigma_i < \frac{r_{iT}}{r_{jT}} \sin \sigma_j$, resulting in $\dot{\psi}_{ij} > 0$. Similarly, in Regions II and III, we have $\sigma_i^* < \sigma_j$, and hence $\sigma_i > \sigma_j$ implies $\sin \sigma_i > \frac{r_{iT}}{r_{jT}} \sin \sigma_j$, resulting in $\dot{\psi}_{ij} < 0$. Therefore, we can summarize the inferences from the current analysis and those in (11) as

$$\begin{aligned} \text{Region I: } \dot{d}_{ij} < 0, \dot{\psi}_{ij} > 0, \text{ if } \sigma_i < \sigma_j, \\ \text{Region II: } \dot{d}_{ij} > 0, \dot{\psi}_{ij} < 0, \text{ if } \sigma_i > \sigma_j, \\ \text{Region III: } \dot{d}_{ij} > 0, \dot{\psi}_{ij} < 0, \text{ if } \sigma_i > \sigma_j, \\ \text{Region IV: } \dot{d}_{ij} < 0, \dot{\psi}_{ij} > 0, \text{ if } \sigma_i < \sigma_j. \end{aligned} \quad (13)$$

It follows from (11) and (13) that inter-pursuer collision can only occur in Regions II and IV during target enclosing. Therefore, no agents in Regions I and III will collide with P_i . This concludes the proof. \square

Lemma 1 shows that the nearby pursuers in Regions I and III will not collide with P_i , so ensuring safety with those pursuers is unnecessary for P_i . This could reduce computational complexity and make the design simpler. Now, we explain why choosing one pursuer from the surrounding pursuers according to (7) is necessary to ensure safety among all pursuers.

Theorem 1 (Inter-pursuer Safety). *The selection of a single nearest colliding pursuer according to (7) and fulfilling the safety condition in (8) is sufficient to guarantee collision avoidance during target enclosing.*

Proof. The essence of this theorem lies in the fact that for any two pursuers, if $d_{ij} > 0$, then the i^{th} pursuer only needs to ensure strict inter-pursuer safety with its nearest colliding neighbor, which can only be present in its Region II. According to the results in Lemma 1, P_i can only collide with the pursuers located in Regions II and IV, and thus the pursuers located in these regions have a tendency to collide with P_i if safety is not ensured. We show that identifying

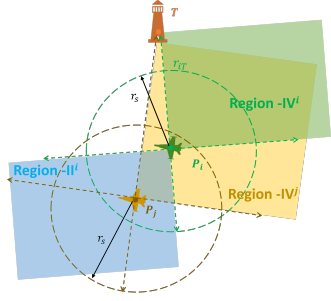


Fig. 7: Engagement with neighboring pursuers in Region II of P_i .

P_i 's nearest colliding neighbor according to (7) enables it to selectively choose a single pursuer from a larger group situated in Region IV, thereby enforcing safety guarantees in the self-organizing swarm, that is, $r_{ij} > 0$ for $i \neq j$.

Let us consider a situation where pursuer P_i has another pursuer, P_j , located within its Region II (denoted as Region I¹), as shown in Fig. 7. Since P_i is the nearest colliding pursuer for P_j , according to (7), P_j must meet the safety criterion in (8) and maneuver accordingly. Hence, P_i can safely approach the desired proximity without colliding with pursuers in its Region II¹. This means that P_i can focus on avoiding collisions with pursuers in its Region IV¹.

Before considering the second scenario, we first analyze the inter-pursuer distance r_{ij} between P_i and P_j to arrive at the nearest colliding pursuer selection criterion discussed in (11). Following (11), we find the values of d_{ij} and ψ_{ij} that minimizes r_{ij} by evaluating the partial derivatives of r_{ij}^2 as in (3) with respect to d_{ij} and ψ_{ij} . We obtain the gradient ∇r_{ij}^2 and Hessian $\nabla^2 r_{ij}^2$ as,

$$\nabla r_{ij}^2 = \begin{bmatrix} \frac{\partial r_{ij}^2}{\partial d_{ij}} \\ \frac{\partial r_{ij}^2}{\partial \psi_{ij}} \end{bmatrix} = \begin{bmatrix} 2d_{ij} + 2r_{iT}(1 - \cos \psi_{ij}) \\ 2r_{iT}^2 \sin \psi_{ij} + 2r_{iT}d_{ij} \sin \psi_{ij} \end{bmatrix}, \quad (14)$$

$$\nabla^2 r_{ij}^2 = \begin{bmatrix} 2 & 2r_{iT} \sin \psi_{ij} \\ 2r_{iT} \sin \psi_{ij} & 2r_{iT}^2 \cos \psi_{ij} + 2r_{iT}d_{ij} \cos \psi_{ij} \end{bmatrix}, \quad (15)$$

It can be readily observed from (3), (14) and (15) that the minimum value of $r_{ij} = 0$ is attained only when $d_{ij} = 0$ and $\psi_{ij} = 0$, since at these values $\nabla r_{ij}^2 = 0$ and $\nabla^2 r_{ij}^2 > 0$ (positive definite). These inferences follow the discussions in Section II-B. From (9), we know that in Region IV of P_i (Region IV¹ in Fig. 7), $d_{ik} > 0$ and $\psi_{ik} < 0$ for an arbitrary pursuer P_k located therein. Therefore, when $r_{ik} \neq 0$, choosing P_k with the smallest d_{ik} and largest ψ_{ik} will select only one pursuer that is closest to P_i in terms of inter-pursuer distance. Our approach ensures safety among pursuers and allows them to self-organize during target enclosing by first picking pursuers located on the nearest loiter circle around the target to minimize d_{ij} . This set of pursuers is denoted by \mathcal{Z}_i , as seen in (6). Next, we select the nearest colliding pursuer with the largest ψ_{ij} from the set \mathcal{Z}_i , fulfilling

the conditions in (7). A pseudocode representation of the algorithm for each pursuer to identify the nearest colliding pursuer is provided in Algorithm 1.

Algorithm 1 Select Nearest Colliding Pursuer

- 1: **Input:** Set of pursuers \mathcal{L} , sensing range r_s , pursuer P_i
 - 2: **Output:** Set of nearest colliding pursuer \mathcal{C}_i
 - 3: Initialize $\mathcal{N}_i \leftarrow \{\}$, $\mathcal{Z}_i \leftarrow \{\}$, $\mathcal{C}_i \leftarrow \{\}$
 - 4: **for** each pursuer $P_j \in \mathcal{L}$ **do**
 - 5: **if** $r_{ij} \leq r_s$ and $d_{ij} > 0$ and $\psi_{ij} < 0$ **then**
 - 6: Add P_j to \mathcal{N}_i
 - 7: **end if**
 - 8: **end for**
 - 9: **for** each pursuer $P_j \in \mathcal{N}_i$ **do**
 - 10: **if** $d_{ij} = \min_{P_k \in \mathcal{N}_i} d_{ik}$ **then**
 - 11: Add P_j to \mathcal{Z}_i
 - 12: **end if**
 - 13: **end for**
 - 14: Select $P_j \in \mathcal{Z}_i$ such that $\psi_{ij} = \max_{P_k \in \mathcal{N}_i} \psi_{ik}$
 - 15: Add P_j to \mathcal{C}_i
-

In the second situation, we consider the presence of multiple pursuers (P_j , P_k and P_l) in Region IV¹, as shown in Fig. 8. Given the scenario, pursuer P_j has the shortest distance to P_i (r_{ij}), while pursuer P_k has the smallest distance between itself and another pursuer (d_{ik}) based on the loiter circles. Additionally, pursuer P_l has the largest inter-pursuer angular spacing between itself and P_i (ψ_{il}). This implies $d_{ik} < d_{ij} < d_{il}$, and $\psi_{il} > \psi_{ij} > \psi_{ik}$. From (7), we can infer that P_k is the nearest colliding pursuer for P_i , who only needs to concern itself with avoiding collision with P_k by executing a suitable maneuver.

For the sake of contradiction, let us consider either P_j or P_l to the nearest colliding pursuer for P_i . First, considering P_j to be the nearest colliding pursuer for P_i , we have $d_{ij} > 0$ based on condition (8), which also implies $d_{il} > 0$. However, this will not ensure $d_{ik} > 0$ and result in a collision between P_i and P_k . Similarly, we can show that selecting P_l as the nearest colliding pursuer will not ensure the prevention of collision of P_i with P_j and P_k , since $d_{il} > 0$ does not imply $d_{ij} > 0$ and $d_{ik} > 0$. Therefore, P_k is the appropriate choice of nearest colliding pursuer chosen as per condition (7), which requires less information than ensuring safety with a pursuer other than the nearest colliding one (which will require additional conditions). By guaranteeing safety condition (8) with respect to P_k , we can infer that $d_{ik} > 0$. This subsequently implies that $d_{ij} > 0$ and $d_{il} > 0$, since P_k is closer to P_i than P_j and P_l . In other words, ensuring that P_i avoids colliding with P_k automatically ensures that P_i avoids colliding with P_j and P_l as well. This concludes the proof. \square

Every pursuer starting away from the target may encounter a nearest colliding pursuer before reaching the desired proximity around the target. Under such a case, the i^{th} pursuer

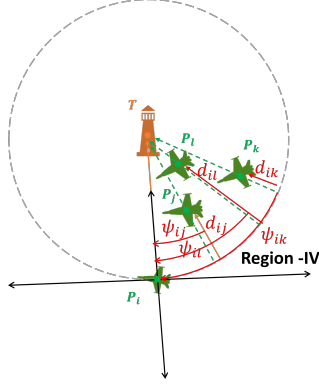


Fig. 8: Engagement with neighboring pursuers in Region IV of P_i .

should maneuver to only avoid collision with its nearest colliding pursuer, ensuring safety conditions in (8). Consequently, this allows the pursuers to settle behind the nearest colliding pursuer on the enclosing orbit, allowing the pursuers to self-organize around the target with inherent safety.

Remark 4. Our methodology capitalizes on the inherent self-organization behavior of each pursuer to adjust their individual trajectory without necessitating explicit cooperation or prior coordination among them. This decentralized approach allows pursuers to operate independently, adapting to changing environmental conditions and avoiding potential collisions while still working towards the collective goal of enclosing the target. By eliminating the need for rigid formations or vehicle-to-vehicle communication, our solution offers a more practical and robust alternative to traditional centralized control strategies.

B. Design of Potential Function

As indicated by the behavior of pursuers observed in Section III, each pursuer must exhibit two distinct behaviors. When there is no nearby colliding pursuer, the i^{th} pursuer's objective is to reach the desired proximity from the target to enclose it. However, if there is a nearest colliding pursuer, the i^{th} pursuer needs to maneuver along a loiter circle with a radius larger than the one corresponding to the nearest colliding pursuer to prevent any potential collisions. These factors enable us to break down the complex multiagent target enclosing problem into more manageable two-body (one pursuer and the target) or three-body (two pursuers and the target) scenarios at any given point in time. Consequently, in this subsection, we present the design of a potential function that will serve as the foundation for developing the target enclosing guidance law.

Let's define the range error for the i^{th} pursuer as,

$$e_i = r_{iT} - r_d, \quad (16)$$

where r_d is the desired fixed proximity from the target such that $\dot{r}_d = 0$. This error variable plays a crucial role in the design of the potential function to ensure inter-pursuer

safety. To analyze the error dynamics, we differentiate e_i with respect to time and use (1a) to obtain the range error rate for the i^{th} pursuer as,

$$\dot{e}_i = \dot{r}_{iT} = -v \cos \sigma_i \quad (17)$$

since $\dot{r}_d = 0$. From the above equation, it is evident that $\dot{e}_i < 0$, if $\sigma_i \in [0, \pi/2)$, which indicates the i^{th} pursuer's motion toward the target, whereas $\dot{e}_i > 0$, represents the opposite case because $\sigma_i \in (\pi/2, \pi]$. The i^{th} pursuer moves on a circle of fixed radius from the target when $\dot{e}_i = 0$ when $\sigma_i = \pi/2$. Therefore, nullifying the range error given in (16), will ensure that the i^{th} pursuer converges to the desired proximity around the target, but additional safety considerations are needed to prevent the inter-pursuer collision.

We propose a potential function for the i^{th} pursuer that incorporates both the required behaviors, which is defined as

$$U_i(e_i, e_j) = \lambda_i \frac{e_i^2}{2} + \eta_i \delta_i e^{-\frac{(e_i - e_j)^2}{2\Delta_i^2}} \quad (18)$$

where λ_i , η_i , and Δ_i are positive scaling constants in the potential function. The subscript j corresponds to $P_j \in C_i$, which is the nearest colliding pursuer corresponding to the i^{th} pursuer. The variable δ_i is a conditional one such that

$$\delta_i = \begin{cases} 1; & \text{if } C_i \neq \emptyset \text{ (} C_i \text{ is not empty),} \\ 0; & \text{otherwise.} \end{cases} \quad (19)$$

The first term in (18) is the attractive component of the potential function, which is active at all times. This term has a unique minimum at $e_i = 0$ and steers the i^{th} pursuer to the desired proximity around the target. The second term in (18) is the repulsive term enabling the i^{th} pursuer to avoid collisions with its nearest colliding pursuer. It is important to note that the latter term is conditional and is only activated based on the existence of the nearest colliding pursuer for P_i , as per the condition given in (19). The first term in (18) is a quadratic term dependent on e_i , whereas the second term (which introduces a repulsive behavior) is a Gaussian function that attains maximum values at $e_i = e_j$ and decreases as $d_{ij} = e_i - e_j$ increases, with this term losing its dominance when $d_{ij} \geq \Delta_i$. If two agents are closer to each other, it is reasonable to assume $d_{ij} < e_i$. Therefore, the first term in (18) will dominate the second term for any selected value of λ_i , η_i and Δ_i if $d_{ij} \gg 0$. However, for small values of d_{ij} , one can select the values of these parameters to ensure that the second term dominates in the region where $d_{ij} = e_i - e_j \in (0, \Delta_i)$. In such a scenario, in the region near the line $e_i - e_j = 0$, the repulsive term dominates the attractive component that will result in P_i moving away from $P_j \in C_i$. Consequently, it follows that there will be a shift in the minimum of the potential function at $e_i = 0$ (for only attractive potential) to $e_i > e_j$ (for combined potential), which allows pursuers to avoid collisions with each other.

To analyze the combined potential function, we compute partial derivatives of (18) with respect to e_i and e_j to obtain the gradient of the potential function as,

$$\frac{\partial U_i}{\partial e_i} = \lambda_i e_i - \frac{\eta_i \delta_i}{\Delta_i^2} e^{-\frac{(e_i - e_j)^2}{2\Delta_i^2}} (e_i - e_j), \quad (20a)$$

$$\frac{\partial U_i}{\partial e_j} = \frac{\eta_i \delta_i}{\Delta_i^2} e^{-\frac{(e_i - e_j)^2}{2\Delta_i^2}} (e_i - e_j). \quad (20b)$$

To obtain the region of minimum potential, we equate (20a)

to zero to obtain, that is, $\lambda_i e_i - \frac{\eta_i \delta_i}{\Delta_i^2} e^{-\frac{(e_i - e_j)^2}{2\Delta_i^2}} (e_i - e_j) = 0$. This above expression is highly nonlinear, and the analytical solution of e_i is difficult to obtain in closed form. The trivial solution is $e_i = 0$ and $e_j = 0$. However, such a situation never arises because when $\delta_i = 1$, $e_i > e_j$. Further, from the above equation, we can infer that the solution to $\frac{\partial U_i}{\partial e_i} = 0$

and $\frac{\partial U_i}{\partial e_j} = 0$, can be given by $e_i - e_j = \epsilon_i$, where ϵ_i denotes a positive value. To verify this, we plot the potential function and the negative gradients for the chosen (typical) values of $\lambda_i = 0.2$, $\eta_i = 100000$ and $\Delta_i = 500$, as depicted in Fig. 9. In Fig. 9, $e_i - e_j > 0$ is the relevant area whenever $\delta_i = 1$. The combined potential is depicted in Fig. 9a, where it is observed that the minimum potential region (depicted by cyan colored region) is situated at $e_i - e_j = \epsilon_i$. Further, in Fig. 9b, the negative gradient lines converge to the line $e_i - e_j = \epsilon_i$. This depicts the existence of a minimum potential point at $e_i = e_j + \epsilon_i$, whenever the repulsive component of the potential is activated.

Remark 5. It is crucial to choose the values of the control parameters λ_i , η_i , and Δ_i judiciously to guarantee that $\epsilon_i > 0$. This ensures that the minimum of the combined potential function in (18) occurs at $e_i > e_j$, leading to $\dot{e}_i > 0$ for all $e_i - e_j \in (0, \epsilon_i)$ and $\dot{e}_i < 0$ for all $e_i - e_j \in (\epsilon_i, \infty)$. Based on (20a), the condition, $\frac{\delta_i}{\Delta_i^2 \lambda_i} > \sup_{t \geq 0} \frac{e_i}{e_i - e_j} e^{-\frac{(e_i - e_j)^2}{2\Delta_i^2}}$, will help select the control parameters to ensure $\epsilon_i > 0$.

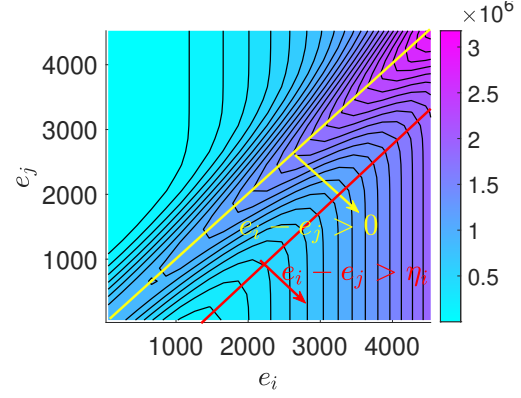
C. Development of the Target Enclosing Guidance Law

In this section, we design the lateral acceleration (control input) for the i^{th} pursuer to steer it on a collision-free path to the desired proximity around the target. To achieve this, we leverage the sliding mode control avowed for its remarkable properties of precision, robustness, and ease of designing, e.g., see [6], [21]–[23], [28], [29].

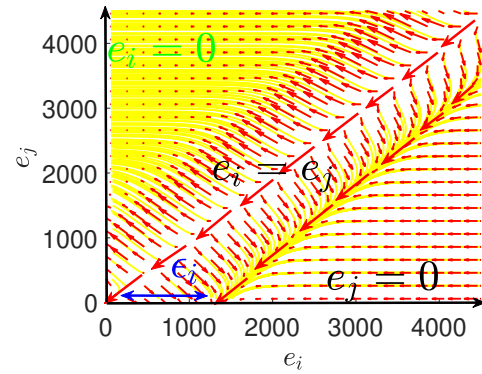
Lemma 2. *The dynamics of the i^{th} pursuer's range error has a relative degree of two with respect to its lateral acceleration.*

Proof. Differentiating \dot{e}_i with respect to time and using (1b), we obtain the dynamics of range error rate as,

$$\ddot{e}_i = \ddot{r}_{iT} = \frac{v^2 \sin^2 \sigma_i}{r_{iT}} + a_i \sin \sigma_i, \quad (21)$$



(a) Potential function U_i .



(b) Gradient lines.

Fig. 9: Potential function and gradient lines for the P_i in presence of a nearest colliding pursuer P_j , with $\lambda_i = 0.2$, $\eta_i = 100000$ and $\Delta_i = 500$.

thereby completing the proof. \square

Inferences from Lemma 2 allow us to construct a suitable sliding manifold for the i^{th} pursuer. To this end, consider the sliding manifold,

$$S_i = \dot{e}_i + \lambda_i e_i - \frac{\eta_i \delta_i}{\Delta_i^2} \exp \left\{ -\frac{(e_i - e_j)^2}{2\Delta_i^2} \right\} (e_i - e_j), \quad (22)$$

on which the i^{th} pursuer's range error rate \dot{e}_i can be driven to the negative gradient $-\nabla_{e_i} U_{ij}$. Note from the above equation that when $\delta_i = 0$ $S_i = \dot{e}_i + \lambda_i e_i$, which is analogous to a second-order sliding manifold with asymptotic error convergence. Further, the last term in (22) represents the collision avoidance term that becomes active when $\delta_i = 1$. We now propose the lateral acceleration (the only control input) for the i^{th} pursuer as,

$$a_i = \frac{1}{\sin \sigma_i} \left[-K_i \text{sign}(S_i) - \frac{v^2 \sin^2 \sigma_i}{r_{iT}} + \lambda_i v \cos \sigma_i + \frac{\delta_i \eta_i v e^{-\frac{(e_i - e_j)^2}{2\Delta_i^2}}}{\Delta_i^2} \left(\frac{(e_i - e_j)^2}{\Delta_i^2} - 1 \right) \cos \sigma_i \right], \quad (23)$$

$$\text{where, } K_i > \frac{\eta_i v}{\Delta_i^2} \left(1 - \frac{r_s^2}{\Delta_i^2}\right) \quad (24)$$

provides a sufficient condition on the controller gain of the i^{th} pursuer. The first term in the above equation drives the pursuers to their respective sliding manifold. The second term represents the centripetal acceleration about the target, while the third term represents the component of its velocity along its LOS with respect to the target. The fourth term in (23) enforces a collision avoidance behavior.

Theorem 2. Consider the equations of relative motion between a single target and multiple pursuers (1), and the i^{th} pursuer-target range error e_i . If the i^{th} pursuer applies the lateral acceleration given in (23), then all the pursuers will self-organize on circle of radius r_d around target without colliding with each other.

Proof. Consider a Lyapunov Function Candidate $V = \sum_{i \in \mathcal{L}} S_i^2$. Differentiating this Lyapunov function with respect to time and using (22), we obtain the dynamics of the sliding manifold as,

$$\dot{V} = \sum_{i \in \mathcal{L}} S_i \dot{S}_i = \sum_{i \in \mathcal{L}} S_i \left(\ddot{e}_i + \lambda_i \dot{e}_i + \frac{\partial^2 U_i}{\partial^2 e_i} \dot{e}_i + \frac{\partial^2 U_i}{\partial^2 e_j} \dot{e}_j \right) \quad (25)$$

Substituting for \ddot{e}_i , $\partial^2 \mathcal{U}_i / \partial^2 e_i$ and $\partial^2 \mathcal{U}_i / \partial^2 e_j$ using (20a), (20b), and (21) in the above expression we obtain,

$$\begin{aligned} \dot{V} = \sum_{i \in \mathcal{L}} S_i & \left[\frac{v^2 \sin^2 \sigma_i}{r_{iT}} + a_i \sin \sigma_i + \lambda \dot{e}_i \right. \\ & \left. + \frac{\eta_i \delta_i e^{-\frac{(e_i - e_j)^2}{2\Delta_i^2}}}{\Delta_i^2} \left(\frac{(e_i - e_j)^2}{\Delta_i^2} - 1 \right) (\dot{e}_i - \dot{e}_j) \right]. \quad (26) \end{aligned}$$

Substituting the proposed lateral acceleration for the i^{th} pursuer given in (23), reduces the above expression to

$$\begin{aligned} \dot{V} &= \sum_{j \in \mathcal{L}} S_j \left[-K_j \text{sign}(S_j) - \frac{\eta_j \delta_j e^{-\frac{(e_i - e_j)^2}{2\Delta_j^2}}}{\Delta_j^2} \left(\frac{(e_i - e_j)^2}{\Delta_j^2} - 1 \right) \dot{e}_j \right], \\ &\leq \sum_{j \in \mathcal{L}} -|S_j| \left[K_j - \frac{\eta_j}{\Delta_j^2} \left| e^{-\frac{(e_i - e_j)^2}{2\Delta_j^2}} \right| |\dot{e}_j| \left| \frac{(e_i - e_j)^2}{\Delta_j^2} - 1 \right| \right], \end{aligned} \quad (27)$$

since $|\dot{e}_j| = v$ and $|e_i - e_j| < r_s$ (as the switching term can be activated only when the colliding vehicle is within the sensing range). The above equation can be further simplified as

$$\dot{V} \leq \sum_{j \in \mathcal{L}} -|S_j| \left[K_j - \frac{\eta_j v}{\Delta_j^2} \left(1 - \frac{r_s^2}{\Delta_j^2}\right) \right], \quad (27)$$

which presents the sufficient condition as given in (24) to ensure, $\dot{V} < 0$, $\forall S_i \in \mathbb{R} \setminus \{0\}$. This implies that S_i 's converge to zero within finite time given by $T^* = |S_i(0)|/K_i$, irrespective whether $\delta_i = 0$ or 1. It is worth mentioning that S_i can suddenly deviate from zero due to the activation/deactivation of the repulsive potential component. However, based on (27), even when S_i shifts suddenly to a non-zero value, S_i will

converge to a zero within a finite time to quickly enforce the sliding mode. Once $S_i = 0$, the pursuers' error rate propagates according to

$$\dot{e}_i = -\lambda_i e_i + \frac{\eta_i \delta_i}{\Delta_i^2} e^{-\frac{(e_i - e_j)^2}{2\Delta_i^2}} (e_i - e_j) = 0. \quad (28)$$

Therefore, once the sliding mode is enforced, P_i may exhibit two distinct behaviors in relation to other vehicles based on the switching term, discussed as Modes 1 and 2 below.

Mode I: When $\delta_i = 0$, indicating the absence of any nearest colliding pursuer for P_i , then the dynamics described in (28) yields $\dot{e}_i = -\lambda_i e_i$. This leads to 1) $\dot{e}_i \leq 0$ when $e_i \geq 0$ and 2) $\dot{e}_i > 0$ when $e_i < 0$. The solution of the range error can be obtained as $e_i(t) = e_i(0)e^{-\lambda_i t}$. Consequently, the pursuer converges to the desired proximity, that is, $r_{iT} \rightarrow r_d$ if λ_i is selected as a positive value.

Mode II: If $\delta_i = 1$, this pertains to the scenario when there exists a nearest colliding neighbor P_j for the pursuer P_i such that $d_{ij} > 0$ and $\psi_{ij} < 0$ at the start of the engagement. In this mode, (28) yields

$$\dot{e}_i = -\lambda_i e_i + \frac{\eta_i}{\Delta_i^2} e^{-\frac{(e_i - e_j)^2}{2\Delta_i^2}} (e_i - e_j) = 0, \quad (29)$$

as $\delta_i = 1$. It can be inferred that the solution of $e_i(t)$ when $\delta_i = 1$ may not be feasible to obtain analytically in each case. However, we can select the values of controller parameters λ_i , η_i and Δ_i to ensure $\dot{e}_i > 0$ when $e_i - e_j < \epsilon_i$ and $\dot{e}_i < 0$ when $e_i - e_j > \epsilon_i$, where $\epsilon_i > 0$ denotes a positive value. This is similar to the behavior of the pursuer under the proposed potential function as discussed earlier in Section III-B. This implies P_i will converge to a loiter circle of radius greater than that of P_j , that is, $e_i \rightarrow e_j + \epsilon_i$ or $r_{iT} \rightarrow r_{jT} + \epsilon_i$. It readily follows from the above relation that $d_{ij} > 0$, which represents the safety condition as in (8). The above condition ensures $d_{ij} > 0$, $\forall t \geq 0$, while $\psi_{ij} < 0$ and $\dot{\psi}_{ij} > 0$ in Region IV of the i^{th} pursuer, as obtained in (13) of Lemma 1. This will result in ψ_{ij} starting from a negative value to become zero. At this moment, P_j will no longer be the nearest colliding neighbor for P_i . Further, if no other vehicle becomes the new nearest colliding neighbor, P_i will undergo the behavior in **Mode I** to reach the desired proximity, settling behind P_j and exhibiting the self-organizing behavior. Otherwise, P_i will undergo the behavior in **Mode II** to avoid collision with the new nearest colliding neighbor and settle behind it. Consequently, every pursuer starting away from the target will alternate between **Mode I** and **Mode II** behaviors, resulting in every pursuer to converge to circle of desired proximity without colliding with other pursuers and organising autonomously on enclosing shape. This concludes the proof. \square

The proposed guidance law (23) is nonsingular even if the term σ_i appears in its denominator, that is, the expression in (23) never becomes unbounded if $\sigma_i \rightarrow 0$ or $\pm\pi$. In the steady state, $\dot{e}_i = -v \cos \sigma_i = 0$ results in $\sigma_i \rightarrow \pm\pi/2$ as the equilibrium points. Therefore, $\sigma_i = 0$ or π are not the equilibrium

points for the pursuers utilizing the proposed guidance law. However, $\sigma_i = 0$ or π may occasionally occur in the transient phase during which a_i will saturate momentarily to drive the system away from such configurations. However, during implementation, control inputs are constrained to remain within finite bounds since the control input values practically cannot be infinite. Therefore, whenever the demand for a_i grows beyond the allowable limits, the control input will saturate and steer the pursuer away from $\sigma_i = 0$ or π .

Remark 6. The control input designed in [Theorem 2](#) is solely based on relative measurements, making it lucrative even in scenarios when global information is not available. The proposed guidance law for the i^{th} pursuer (23) is independent of the other pursuers' motion, thereby exhibiting robustness to their movement.

Remark 7. Ensuring the expression of K_i as in (24) is greater than zero provides an additional condition on the selection of the control parameters, that is, $\Delta_i > r_s$. This simply implies that the region of the dominance of the repulsive term denoted by Δ_i is greater than the i^{th} pursuer's sensing radius, resulting in the repulsive field dominating within the sensing radius. This will enable the pursuers to move out of the sensing range of their respective nearest colliding pursuers to avoid colliding with them, such that at steady state, none of the pursuers are situated in each other's sensing radius.

IV. SIMULATION RESULTS

In this section, we demonstrate the efficacy of the proposed control law in autonomously organizing the pursuers to enclose a stationary target. In the following results, the target is stationary at the position $[x_T \ y_T] = [0, 0]^T$ m. All pursuers start at a different distances from the target and move at a constant speed of 40 m/s and. The initial position of pursuers are denoted by square markers in the subsequent trajectory plots. The desired proximity from the target is set as $r_d = 100$ m for all the simulation results. The controller gains and other parameters are selected as follows: $K_i = 10$, $\lambda_i = 0.9$, $\eta_i = 70000$, $\Delta = 100$, and $r_s = 50$ m.

The first set of results illustrates the scenario in which six pursuers start away from the target, as depicted in [Fig. 10](#). The initial arrangement of the pursuers around the target in a clockwise direction is given as $P_2 - P_1 - P_3 - P_4 - P_5 - P_6$, as shown by square markers in the figure. It is observed that the final arrangement of the pursuers on the desired proximity (as depicted by circular markers) is given as, $P_2 - P_3 - P_1 - P_4 - P_6 - P_5$. This indicates that only P_3 and P_6 encounter a nearest colliding pursuer and reorganize to avoid collision. Meanwhile, the $P_1, P_2, P_4, \text{ and } P_5$ move directly to the desired proximity without encountering the nearest colliding pursuer. The profiles of the error variables and sliding manifold are depicted [Fig. 10b](#), where the sliding manifold converges to zero within a finite time. The profiles of S_i for only P_3 and P_6 depict sudden deviations at different instances of time, which represent the instance of activation/deactivation of the collision avoidance component

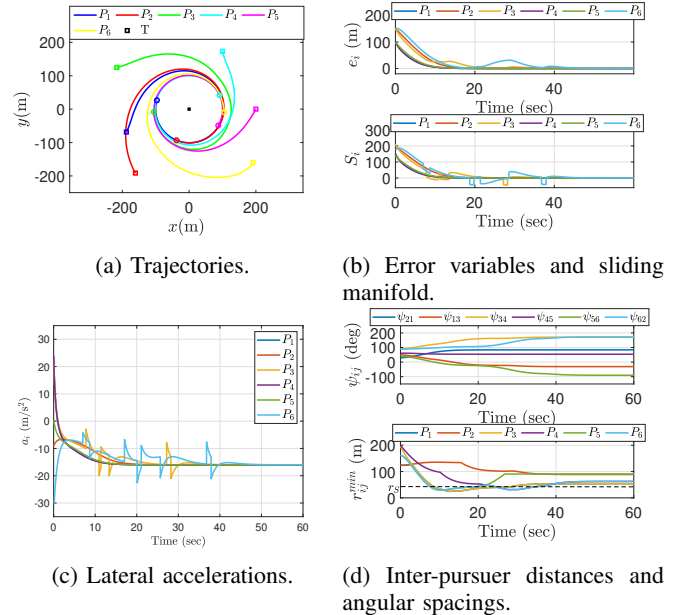


Fig. 10: Collision-free self-organising target enclosing with 6 pursuers.

of the control input. Note that whenever collision avoidance is activated, the range error diverges from zero momentarily to ensure safety.

[Fig. 10c](#) depicts the profiles of lateral accelerations of the pursuers converging to the same constant value at a steady state, as all the pursuers eventually converge to the same loiter circle of radius of desired proximity. The lateral acceleration profiles of P_3 and P_6 vary from the other pursuers due to the activation of the collision avoidance component. Finally, the profiles of inter-pursuer variables are shown in [Fig. 10d](#), where the profiles of ψ_{ij} change sign crossing zero for only P_3 and P_6 . This shows that these pursuers have autonomously reorganized from their initial configurations, where the profiles r_{ij}^{\min} depict that the distance between the two closest pursuers never reaches zero. Further, at steady state, all the pursuers have $r_{ij}^{\min} > r_s$, which implies that all the pursuers only converge to the desired proximity when the sensing range of no two pursuers intersect. Therefore, all the pursuers have only the attractive component of the control input activated at the steady state.

[Fig. 11](#) illustrates the second set of results where initially, four pursuers (P_1 to P_4) are already moving on the circle of desired proximity when two other pursuers (P_5 and P_6) start away from the desired proximity. From the [Figures 11a to 11c](#), it is evident that P_5 reaches the desired proximity without encountering a nearest colliding pursuer and autonomously organizing on the free space on the enclosing shape. While P_5 itself becomes the nearest colliding pursuer for P_6 , resulting in P_6 taking a larger route to converge to the desired proximity behind P_6 . This is verified by [Fig. 11d](#), where only the profiles related to P_6 exhibit abrupt variation

compared to other pursuers, indicating to activation of the repulsive component of the control input. Therefore, P_5 and P_6 are able to autonomously join the enclosing formation without colliding with other pursuers.

Furthermore, we offer video demonstrations of our simulation results, accessible at [this link](#). The videos titled “results_1.mp4” and “results_2.mp4” showcase the simulation outcomes corresponding to the scenarios presented in the paper. Additionally, “results_3.mp4” and “results_4.mp4” illustrate the self-organizing target enclosing in large swarms with 10 and 20 pursuers, respectively.

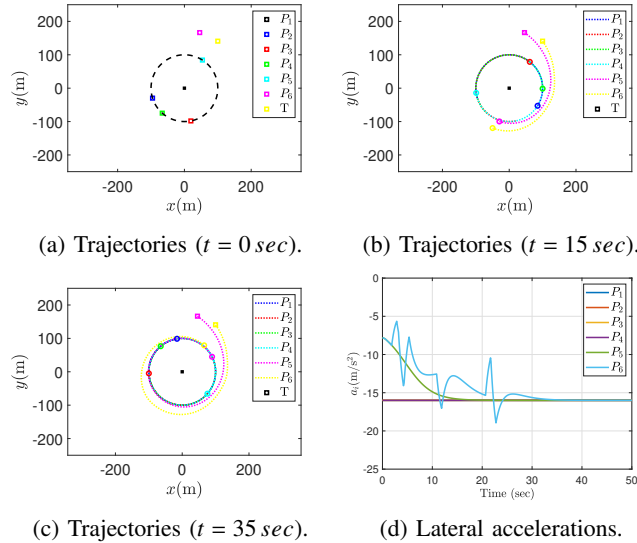


Fig. 11: Two pursuers joining the enclosing formation.

V. CONCLUSIONS

In this paper, we proposed guidance laws for multiple pursuers to safely and autonomously organize at the desired proximity to encircle a stationary target, using only the relative information. In our approach, the agents are free to converge to any point on the enclosing shape as long as they maintain a safe distance between them, which may result in the pursuers not requiring a pre-determined formation structure and autonomously organizing on the enclosing shape. Our guidance strategy ensures that each pursuer selects at most one other pursuer based on certain collision conditions. We show that preventing collision with the selected other pursuer is sufficient to avoid collisions with all the other pursuers. To tailor the desired switching behavior required, we proposed a potential function such that the attractive component of the potential is activated all the time. Meanwhile, the repulsive component is activated whenever the pursuer encounters a nearest colliding pursuer. Further, we utilized sliding mode control to develop the reaching law, ensuring finite time convergence of the sliding manifold, followed by asymptotic convergence of the error to zero. The resulting guidance law enables pursuers

to move towards the desired proximity along collision-free paths, offering increased maneuvering flexibility, requiring minimal information, and demonstrating robustness to the motion of other pursuers. Validation of the guidance laws with different numbers of pursuers attests to the merits of the proposed guidance algorithm. Potential future extensions of this work may involve incorporating a moving target, exploring three-dimensional spaces, and integrating obstacle avoidance techniques.

REFERENCES

- [1] P. Kumar Ranjan, A. Sinha, Y. Cao, D. Tran, D. Casbeer, and I. Weintraub, “Energy-efficient ring formation control with constrained inputs,” *Journal of Guidance, Control, and Dynamics*, vol. 46, no. 7, pp. 1397–1407, 2023.
- [2] P. Iscold, G. A. S. Pereira, and L. A. B. Torres, “Development of a hand-launched small uav for ground reconnaissance,” *IEEE Transactions on Aerospace and Electronic Systems*, vol. 46, no. 1, pp. 335–348, 2010.
- [3] H. Huang, A. V. Savkin, and C. Huang, “Decentralized autonomous navigation of a uav network for road traffic monitoring,” *IEEE Transactions on Aerospace and Electronic Systems*, vol. 57, no. 4, pp. 2558–2564, 2021.
- [4] Y. Wang, T. Kirubarajan, R. Tharmarasa, R. Jassemi-Zargani, and N. Kashyap, “Multiperiod coverage path planning and scheduling for airborne surveillance,” *IEEE Transactions on Aerospace and Electronic Systems*, vol. 54, no. 5, pp. 2257–2273, 2018.
- [5] Z. Mei, X. Shao, Y. Xia, and J. Liu, “Enhanced fixed-time collision-free elliptical circumnavigation coordination for uavs,” *IEEE Transactions on Aerospace and Electronic Systems*, pp. 1–14, 2024.
- [6] A. Sinha and Y. Cao, “Three-dimensional autonomous guidance for enclosing a stationary target within arbitrary smooth geometrical shapes,” *IEEE Transactions on Aerospace and Electronic Systems*, vol. 59, no. 6, pp. 9247–9256, 2023.
- [7] A. Sinha and Y. Cao, “3-d nonlinear guidance law for target circumnavigation,” *IEEE Control Systems Letters*, vol. 7, pp. 655–660, 2023.
- [8] T.-H. Kim and T. Sugie, “Cooperative control for target-capturing task based on a cyclic pursuit strategy,” *Automatica*, vol. 43, no. 8, pp. 1426–1431, 2007.
- [9] J. A. Marshall, M. E. Broucke, and B. A. Francis, “Pursuit formations of unicycles,” *Automatica*, vol. 42, no. 1, pp. 3–12, 2006.
- [10] E. W. Frew, D. A. Lawrence, and S. Morris, “Coordinated standoff tracking of moving targets using lyapunov guidance vector fields,” *Journal of Guidance, Control, and Dynamics*, vol. 31, no. 2, pp. 290–306, 2008.
- [11] A. A. Pothan and A. Ratnoo, “Curvature-constrained lyapunov vector field for standoff target tracking,” *Journal of Guidance, Control, and Dynamics*, vol. 40, no. 10, pp. 2729–2736, 2017.
- [12] H. Oh, S. Kim, H.-s. Shin, B. A. White, A. Tsourdos, and C. A. Rabbath, “Rendezvous and standoff target tracking guidance using differential geometry,” *Journal of Intelligent & Robotic Systems*, vol. 69, pp. 389–405, 01 2013. Copyright - Springer Science+Business Media Dordrecht 2013; Last updated - 2014-08-23.
- [13] A. T. Hafez, A. J. Marasco, S. N. Givigi, M. Iskandarani, S. Yousefi, and C. A. Rabbath, “Solving multi-uav dynamic encirclement via model predictive control,” *IEEE Transactions on Control Systems Technology*, vol. 23, no. 6, pp. 2251–2265, 2015.
- [14] X. Shao, Y. Xia, Z. Mei, and W. Zhang, “Model-guided reinforcement learning enclosing for uavs with collision-free and reinforced tracking capability,” *Aerospace Science and Technology*, p. 108609, 2023.
- [15] Y. Cao, “Uav circumnavigating an unknown target under a gps-denied environment with range-only measurements,” *Automatica*, vol. 55, pp. 150–158, 2015.
- [16] F. Dong, K. You, and S. Song, “Target encirclement with any smooth pattern using range-based measurements,” *Automatica*, vol. 116, p. 108932, 2020.
- [17] F. Dong, K. You, L. Xie, and Q. Hu, “Coordinate-free circumnavigation of a moving target via a pd-like controller,” *IEEE Transactions on Aerospace and Electronic Systems*, vol. 58, no. 3, pp. 2012–2025, 2022.

- [18] S. Park, "Circling over a target with relative side bearing," *Journal of Guidance, Control, and Dynamics*, vol. 39, no. 6, pp. 1454–1458, 2016.
- [19] S. Park, "Guidance law for standoff tracking of a moving object," *Journal of Guidance, Control, and Dynamics*, vol. 40, no. 11, pp. 2948–2955, 2017.
- [20] P. Jain, C. K. Peterson, and R. W. Beard, "Encirclement of moving targets using noisy range and bearing measurements," *Journal of Guidance, Control, and Dynamics*, vol. 45, no. 8, pp. 1399–1414, 2022.
- [21] P. K. Ranjan, A. Sinha, and Y. Cao, "Robust uav guidance law for safe target circumnavigation with limited information and autopilot lag considerations," *AIAA SCITECH 2024 Forum*, 2024.
- [22] A. Sinha and Y. Cao, "Three-dimensional guidance law for target enclosing within arbitrary smooth shapes," *Journal of Guidance, Control, and Dynamics*, vol. 46, no. 11, pp. 2224–2234, 2023.
- [23] A. Sinha and Y. Cao, "Nonlinear guidance law for target enclosing with arbitrary smooth shapes," *Journal of Guidance, Control, and Dynamics*, vol. 45, no. 11, pp. 2182–2192, 2022.
- [24] Y. Lan, G. Yan, and Z. Lin, "Distributed control of cooperative target enclosing based on reachability and invariance analysis," *Systems & Control Letters*, vol. 59, no. 7, pp. 381–389, 2010.
- [25] A. Franchi, P. Stegagno, and G. Oriolo, "Decentralized multi-robot encirclement of a 3d target with guaranteed collision avoidance," *Autonomous Robots*, vol. 40, pp. 245–265, 2016.
- [26] K. Lu, S.-L. Dai, and X. Jin, "Cooperative constrained enclosing control of multirobot systems in obstacle environments," *IEEE Transactions on Control of Network Systems*, pp. 1–12, 2023.
- [27] R. Sharma and D. Ghose, "Collision avoidance between uav clusters using swarm intelligence techniques," *International Journal of Systems Science*, vol. 40, no. 5, pp. 521–538, 2009.
- [28] V. Utkin, S. Drakunov, H. Hashimoto, and F. Harashima, "Robot path obstacle avoidance control via sliding mode approach," in *Proceedings IROS '91:IEEE/RSJ International Workshop on Intelligent Robots and Systems '91*, pp. 1287–1290 vol.3, 1991.
- [29] V. Gazi, "Swarm aggregations using artificial potentials and sliding-mode control," *IEEE Transactions on Robotics*, vol. 21, no. 6, pp. 1208–1214, 2005.